Inorg. Chem. **1992,** *31,* 3007–3010

Articles

Theoretical Study of Bonding and Electrical Conductivity in Compounds with the NbAs$_2$ Structure

Pere Alemany[†] and Santiago Alvarez*

Departament de Química Inorgànica, Universitat de Barcelona, Diagonal 647, 08028 Barcelona, Spain

Received December 17, 1991

The electronic structure of NbAs$_2$ has been studied by means of band electronic structure calculations within the extended Hückel framework. A delocalized picture of the electronic structure emerges, which cannot be expressed in terms of the Zintl rules. NbAs$_2$ is found to be metallic in character but with a low density of states at the Fermi level. Possible relationships between the band structure and the existence of superconductivity at low temperature for the isostructural compound MoAs$_2$ are discussed in light of the BCS (Bardeen–Cooper–Schrieffer) theory.

The transition metal pnictides can be roughly classified in two families according to their structural characteristics.[1] The first family includes pnictide-rich compounds, mainly of the late transition metals, whose structures can be described in terms of two-electron bonds, thus permitting clear-cut predictions of their electrical and magnetic properties. The metal atoms usually present octahedral or tetrahedral coordination spheres of pnictide ions. The pnictide atoms may be bonded to each other in an anionic sublattice in which every atom is tetrahedrally coordinated.

The second family is formed by metal-rich compounds. The coordination numbers of both the metal and pnictide atoms are usually high, and the bonding, in the borderline between covalent and metallic, cannot be interpreted in terms of two-electron bonds. Therefore, the assignment of formal oxidation states and the predictions of electrical or magnetic behavior based on their crystal structures are dubious. The main difficulty stems from the large number of interatomic contacts shorter than the van der Waals distance and from the resulting ambiguity in the assignment of formal charges.

To the latter family belong those compounds which crystallize in the NbAs$_2$ structure,[2–5] sometimes also described as the OsGe$_2$ structure.[6] The transition metal pnictides with the NbAs$_2$ structure, belonging to groups 5 and 6, are displayed in Table I, together with their electrical and magnetic properties. All of them are metallic, and two become superconductors below 1 K (MoAs$_2$ and WAs$_2$). It is noteworthy that superconductivity has been found for the arsenides of group 6 but not for those of group 5 metals.

In an attempt to provide an approximate description of the bonding and formal oxidation states in the NbAs$_2$ structure, and an explanation for their electrical properties, including the problem of whether the conduction path is metal- or pnictide-centered, we have undertaken a band electronic structure study of NbAs$_2$ within the extended Hückel formalism (see Appendix for computational details).

Crystal Structure

Previous to a discussion of its electronic structure, an outline of the salient features of the NbAs$_2$ structure is needed. The structure of NbAs$_2$ is monoclinic (space group *C*2), with four Nb atoms per unit cell occupying two crystallographically independent positions.[5] The simplest description of the structure is a metal-centered one: each niobium atom is surrounded by six arsenic atoms in a trigonal prismatic arrangement with two additional arsenic atoms of neighboring prisms (crystallographic directions *a* and *c*) capping two tetragonal faces. Two such bicapped trigonal prisms share their third tetragonal faces (**1**) forming a Nb–Nb bond.[20] To complete the structure, the prisms are stacked along the crystallographic *b* direction through their trigonal faces. A projection of the resulting structure on the *ac* plane is shown in Figure 1, with the main interatomic distances collected in Table II. The capping bonds are labeled *r* and *s* in Figure 1. The resulting arrangement of trigonal prisms has several As–As contacts at varying distances (bonds *t*–*w* in Figure 1 and Table II).

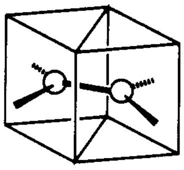

1

It is reasonable to admit that the As–As contacts of type *t* (2.45 Å) are actually chemical bonds and correspondingly half of the arsenic atoms are forming As$_2^{4-}$ pairs. If we consider longer As–As distances to be nonbonding, the remaining As atoms could be considered as As^{3-} ions. This leaves us with Nb^{5+} (4d^0 configuration), consistent with the diamagnetism but unable to explain the existence of Nb–Nb bonds or the metallic conductivity.

[†] Current address: Department of Chemistry, Cornell University, Ithaca, NY.

(1) Hulliger, F. *Struct. Bonding* **1968**, *4*, 63.
(2) Furuseth, S.; Kjekshus, A. *Nature* **1964**, *203*, 512.
(3) Furuseth, S.; Kjekshus, A. *Acta Chem. Scand.* **1964**, *18*, 1180.
(4) Saini, G. S.; Calvert, L. D.; Taylor, J. B. *Can J. Chem.* **1964**, *42*, 630.
(5) Furuseth, S.; Kjekshus, A. *Acta Crystallogr.* **1965**, *18*, 320.
(6) Weitz, G.; Born, L.; Hellner, E. *Z. Metallk.* **1960**, *51*, 238.
(7) Hulliger, F. *Nature* **1964**, *204*, 775.
(8) Gölin, M.; Carlsson, B.; Rundquist, S. *Acta Chem. Scand.* **1975**, *A29*, 706.
(9) Rundqvist, S. *Nature* **1966**, *211*, 847.
(10) Furuseth, S.; Selte, K.; Kjekshus, A. *Acta Chem. Scand.* **1965**, *19*, 95.
(11) Ling, R. G.; Belin, C. *C. R. Acad. Sci. Paris, Ser. 2* **1981**, *292*, 891.
(12) Jeitschko, W.; Donohue, P. C. *Acta Crystallogr.* **1973**, *B29*, 783.
(13) Jensen, P.; Kjekshus, A. *Acta Chem. Scand.* **1964**, *18*, 1798. Jensen, P.; Kjekshus, A.; Skansen, T. *Acta Chem. Scand.* **1966**, *20*, 403.
(14) Taylor, J. B.; Calvert, L. D.; Hunt, M. R. *Can. J. Chem.* **1965**, *43*, 3045.
(15) Brown, A. *Nature* **1965**, *206*, 502.
(16) Rühl, R.; Jeitschko, W. *Monatsh. Chem.* **1983**, *114*, 817.
(17) Roberts, B. W. *J. Phys. Chem. Ref. Data* **1976**, *5*, 581.
(18) Andres, K.; Hull, G. W., Jr.; Hulliger, F. *J. Mater. Sci.* **1972**, *7*, 344.
(19) Parthé, E. *Acta Crystallogr.* **1963**, *16*, 71.
(20) The Nb–Nb distance corresponds roughly to those of unambiguous single bonds: Alemany, P.; Alvarez, S.; Zubkov, V. G.; Zhukov, V. P.; Pereliaev, V. A.; Kontsevaya, I.; Tyutyunnik, A. Submitted for publication.

0020-1669/92/1331-3007$03.00/0

Table I. Electric and Magnetic Properties of Transition Metal Pnictides with the $NbAs_2$ Structure[a]

cpd	struct ref	electric conduct	magnetism	ref
VP_2	7, 8	$T_n = 1.1$ K	const paramag	1
VAs_2	7	$T_n = 0.33$ K	const paramag	1, 17
NbP_2	7, 9	$T_n = 1.1$ K		1
$NbAs_2$	2–5	$T_n = 0.012$ K	diamag	2, 3, 18
$NbSb_2$	2, 3, 5	$T_n = 0.30$ K	diamag	2, 3, 18
TaP_2	6, 7	$T_n = 1.1$ K	const paramag	1
$TaAs_2$	4, 10, 11	$T_n = 0.035$ K	diamag	1, 10, 18
$TaSb_2$	10	$T_n = 0.30$ K	diamag	7, 10, 18
CrP_2	12	$T_n = 4.2$ K	diamag	12
$CrAs_2$	12	$T_n = 4.2$ K		12
$MoAs_2$	7, 13–15	$T_c = 0.41$ K	diamag	13, 18
α-WP_2	7, 9, 16	$T_n = 0.33$ K	diamag	1, 18
WAs_2	7, 14	$T_c = 0.9$ K	diamag	13, 17–19

[a] All compounds are metallic. T_c is the critical temperature for superconductivity, and T_n is the lowest temperature at which superconductivity was not found.

Table II. Bond Distances (Å) in $NbAs_2$ and $MoAs_2$, Calculated from Crystal Data in Refs 5 and 15, Respectively

bond		$NbAs_2$	$MoAs_2$
M–M	*a*	3.01	3.00
M–As	*r*	2.66	2.59
	s	2.74	2.68
	prism	2.54	2.52
	prism	2.66	2.61
	prism	2.70	2.72
As–As	*t*	2.45	2.41
	u	2.84	2.75
	v	3.05	2.93
	w	2.98	2.95

In an alternative description, all As–As distances shorter than 3.0 Å can be considered as bonds. All As atoms would be zerovalent and bonded to three other As atoms. This approach provides us with an alternative description of the structure: the As atoms form layers parallel to the *ab* plane. In the projection of Figure 1, bonds *t* and *u* correspond to one layer and bonds *w* and *v* to another layer. Between such layers are sandwiched the Nb^0 atoms ($4d^5$ configuration). In such case, the diamagnetism is not easy to explain, and the electron count around each Nb atom is 21, neglecting contributions from Nb–Nb bonds, clearly violating the 18-electron rule. Obviously, the real electronic structure should lie somewhere between both extreme situations, and a delocalized description is needed.

Band Electronic Structure

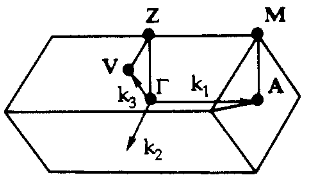

2

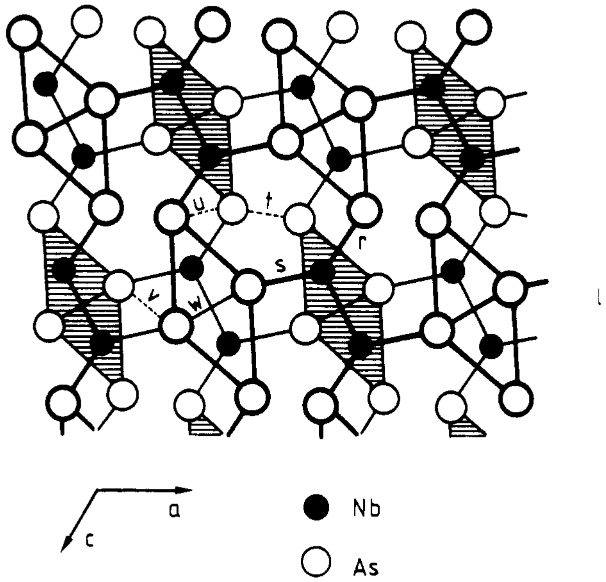

Figure 1. Projection of the $NbAs_2$ structure onto the *ac* plane. The shaded prisms are displaced by *c*/2 relative to the unshaded ones. The labels *r* and *s* indicate different Nb–As distances, and *t*–*w* identify As--As distances.

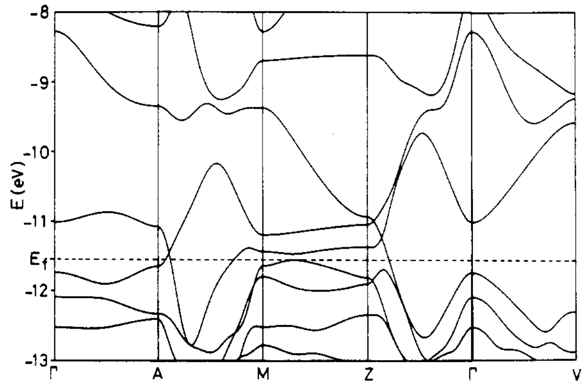

Figure 2. Dispersion relationships of $NbAs_2$ along selected lines of the Brillouin zone (**2**).

The band calculations (see Appendix for details) have been carried out using the primitive unit cell containing two formula units. The translation vectors of the primitive cell are $t_1 = c$, $t_2 = (a - b)/2$, and $t_3 = (a + b)/2$, and the corresponding Brillouin zone is represented in **2**. The dispersion relationships along several lines of the Brillouin zone[21] are shown in Figure 2, where the metallic character of $NbAs_2$ is evident. There are bands crossing the Fermi level ($\mathscr{E}_F = -11.52$ eV) along the ΓZ and AM lines, but not along the ΓA, MZ, and ΓV lines of the BZ. This suggests that the conductivity must be anisotropic, with its largest value along the stacks of prisms (crystallographic *b* direction). Since the Nb–Nb distance in this direction is relatively long (3.38 Å), the mixing of Nb and As orbitals is crucial for the dispersion of such bands, and hence for the electrical conductivity.

The large slopes of the bands across the Fermi level are also indicative of a small effective mass for the conduction electrons, i.e., a good electrical conductivity.[22] There are few levels around the Fermi energy, not only along the lines represented in Figure 2 but also throughout the BZ as seen in the density of states (DOS) plot of Figure 3. As a result, a valley with a small density of states appears around $\mathscr{E}_F$.

In the DOS plot (Figure 3), the shaded area indicates the contribution of the Nb atomic orbitals. The band levels close to $\mathscr{E}_F$ are clearly metal centered and correspond mainly to d orbitals. It must be also stressed that there is an important participation of the metal atomic orbitals in the occupied band levels (larger than 30% of the Nb orbitals, as indicated by the contribution to the DOS integrated up to $\mathscr{E}_F$), thus indicating that a formal oxidation state of Nb^{5+} gives a rather poor description of the electronic structure.

---

(21) For a detailed study of the band structure of the structure of NbPS, with bicapped, fused prisms connected in a different way, see: Keszler, D. A.; Hoffmann, R. *J. Am. Chem. Soc.* **1987**, *109*, 118.

(22) Cox, P. A. *The Electronic Structure and Chemistry of Solids*; Oxford University Press: Oxford, U.K., 1987.

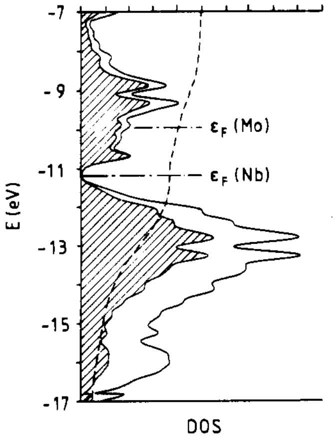

Figure 3. Density of states (DOS) plot for NbAs$_2$, contribution of the Nb atoms to the total DOS (shaded area), and integrated DOS for the Nb atoms (dashed line). The Fermi levels indicated for NbAs$_2$ and MoAs$_2$ were calculated within the rigid-band approximation.

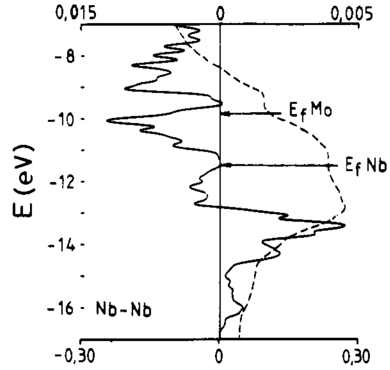

Figure 4. COOP curve for the Nb–Nb interaction. Positive values indicate bonding interaction; negative values, antibonding interaction (the values at the top of each curve correspond to the full scale of the corresponding COOP). The dashed line represents the integrated overlap population (the full scale corresponds to the values indicated at the bottom).

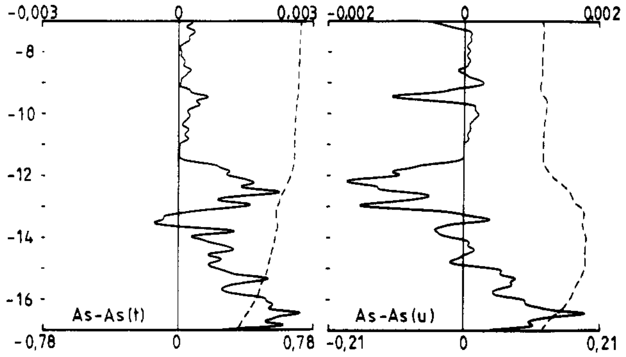

Figure 5. COOP curves for the As–As interactions of types *t* and *u* (see Figure 1). All settings are as in Figure 4.

Let us now look at the bonding with the help of the COOP curves[23] (Figures 4–6). Consider first Nb–Nb interactions (Figure 4): most of the levels below $\mathcal{E}_F$ are Nb–Nb bonding, giving an atomic overlap population of 0.232, clearly indicating the existence of Nb–Nb bonding.[24]

Assuming a rigid-band approximation, the Fermi level for MoAs$_2$ is calculated at −9.83 eV, thus occupying metal–metal antibonding levels which are empty in NbAs$_2$. The fact that the Mo–Mo bond distance in MoAs$_2$ (3.00 Å) is practically identical to the Nb–Nb one (3.01 Å) in NbAs$_2$, given its smaller atomic radius, may be indicative of a slightly weaker metal–metal bond, in agreement with the calculated COOP curve. A similar trend is found for each pair of structures of a group 5 and a group 6 pnictide (Table III).

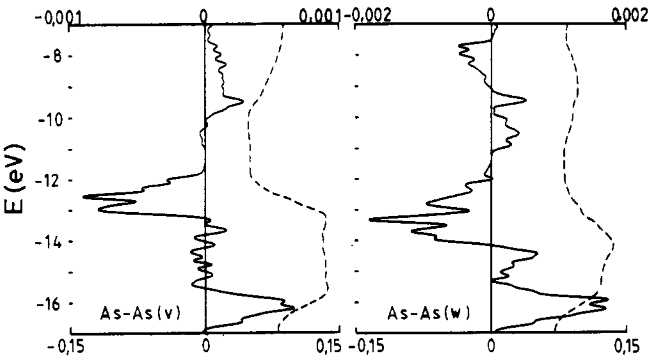

Figure 6. COOP curves for the As–As interactions of types *v* and *w* (see Figure 1). All settings are as in Figure 4.

Table III. Metal Ionic Radii and M–M Bond Distances (Å) in Compounds with the NbAs$_2$ Structure

cpd	r_M	d_{M-M}	cpd	r_M	d_{M-M}
VP$_2$	1.35	2.79	CrP$_2$	1.29	2.78
VAs$_2$		2.88			
NbP$_2$	1.47	2.89			
NbAs$_2$		3.00	MoAs$_2$	1.40	2.98
NbSb$_2$		3.24			
TaP$_2$	1.47	2.88	WP$_2$	1.41	2.82
TaAs$_2$		3.06	WAs$_2$		2.95
TaSb$_2$		3.28			

If we look now at the short As–As bond (t = 2.45 Å, Figure 1), its COOP curve (Figure 5) shows a large integrated overlap population value (0.670) up to the NbAs$_2$ Fermi level. On the other hand, the remaining As–As contacts (u–w) have both bonding and antibonding levels below the Fermi energy (Figures 5 and 6) and their integrated COOP's for the occupied levels are positive but small (0.126, 0.081, and 0.049 for bonds u, w, and v, respectively), in excellent agreement with the longer experimental distances (2.84, 2.97, and 3.05 Å, respectively). However, it must be considered that, other things being equal, the overlap population (OP) calculated at a longer distance is per force smaller. In order to sort out the effect of the experimental bond distances and of the electronic factors on the calculated overlap populations, we have calculated the As–As OP as a function of the interatomic distance in the hypothetical molecule $As_2H_6^{2+}$ with an staggered conformation (Figure 7). The OP calculated for the t bonds in the NbAs$_2$ structure is practically the same as that for the model molecule with the same bond distance, whereas the calculated OP's for bonds u–w are much smaller than expected for *true bonds* with the same As–As distances. It can be therefore concluded that the As–As pairs of type t are chemical bonds, whereas the longer distances (u–w) correspond to nonbonded interactions. In the COOP curves (Figures 5 and 6) is seen that adding one electron, as in MoAs$_2$, has little effect on the As–As OP's, and the systematic diminution of the As–As distances from NbAs$_2$ to MoAs$_2$ should probably be attributed to the shorter M–As distances (Table II), consistent with the smaller atomic radius of Mo (Table III). It is also interesting to observe that the additional electrons present in MoAs$_2$ occupy levels which are essentially As–As nonbonding, as expected for metal-centered levels (Figure 3). Hence, the arsenic sublattice is practically invariant between NbAs$_2$ and MoAs$_2$ (see Table II).

Electronic Structure and Superconductivity of MoAs$_2$

As discussed above (see Table I), the arsenides of Mo and W become superconductors at 0.4 and 0.9 K, respectively, while NbAs$_2$ does not show superconductivity down to 0.012 K.[18]

---

[23] For an introduction to the DOS and COOP curves see, e.g.: Hoffmann, R. *Solids and Surfaces. A Chemist's View of Bonding in Extended Structures*; VCH Publishers: New York, 1988. See also ref 22.

[24] For a discussion on the Nb–Nb bond order/bond distance relationships, see ref 20.

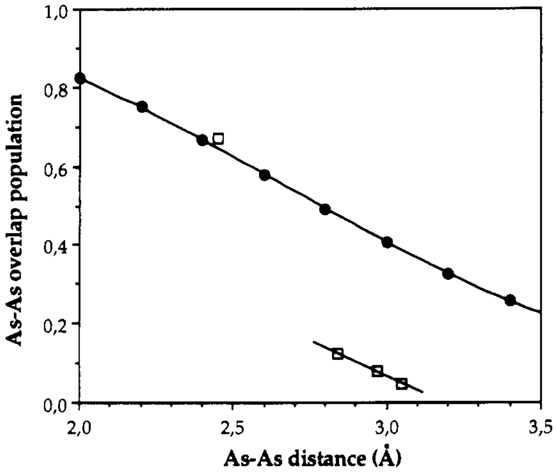

Figure 7. As–As overlap population as a function of the As–As distance calculated for $As_2H_6^{2+}$ (circles). The As–As overlap populations calculated for the different pairs of arsenic atoms (*t*–*w*) in $NbAs_2$ in the experimental structure are represented by squares.

According to the BCS theory,[25] the T_c of superconductivity is related to the density of states at the Fermi level, $N(\mathcal{E}_F)$, according to the equation

$$T_c \propto \langle \omega \rangle \exp\left[\frac{-1}{N(\mathcal{E}_F)\,V}\right]$$

where ω is the average phonon frequency (related to the Debye temperature) and V is the pairing potential arising from electron–phonon interaction. Since $NbAs_2$ and $MoAs_2$ are isostructural, no significant differences in their Debye temperatures are expected, and the experimental ratio $T_c(MoAs_2)/T_c(NbAs_2) > 40$ should be ascribed to the exponential factor. One of the variables in the exponential part is the density of states at the Fermi level, which can be roughly estimated from our calculations. Given the electronic structure discussed above, with the Fermi level of $NbAs_2$ in a pseudogap, and assuming a rigid-band approach, the density of states at the Fermi level for $MoAs_2$ (see Figure 3) is roughly 30 times larger than that of $NbAs_2$. Hence, the absence of superconductivity in $NbAs_2$ may be associated with the low density of states at the Fermi level. Adding electrons to, or subtracting electrons from, $NbAs_2$ should drastically increase $N(\mathcal{E}_F)$, eventually reaching a measurable T_c. The study of nonstoichiometric derivatives of the type $M_xNb_{1-x}As_2$ (M = Zr, Mo) may provide a test for the relationship between $N(\mathcal{E}_F)$ and T_c in this family of compounds.

The second variable in the exponential expression of T_c is related to the electron–phonon coupling interaction and can be best seen in the expression derived by McMillan[26]

$$T_c \propto \Theta \exp\left[-\frac{1}{\lambda - \mu^*}\right]$$

where Θ is the Debye temperature, μ^* is the Coulomb pseudopotential of Morel and Anderson,[27] and λ is the dimensionless electron–phonon coupling constant, related to the frequency of the coupled phonon (ω) and to the atomic mass (for the simplest lattice with one atom per unit cell) as follows:

$$\lambda = \frac{N(\mathcal{E}_F)\,\langle I^2 \rangle}{M\langle \omega^2 \rangle}$$

where $\langle I^2 \rangle$ is the electron–phonon coupling integral averaged over the Fermi surface. Since the crystal orbitals around the Fermi level are metal centered and metal–metal antibonding, the phonon effective for electron–phonon coupling must involve metal–metal stretchings. According to the COOP curve for the Nb–Nb bonds (Figure 4), these are stronger than the Mo–Mo ones; hence, the $NbAs_2$ lattice must be stiffer than the $MoAs_2$ one and the phonon frequencies important for superconductivity are expected to be higher for $NbAs_2$ than for $MoAs_2$. The mass effect, on the other hand, must be negligible, given the small difference in atomic weights between both metals. Consequently, λ must be smaller for $NbAs_2$ than it is for $MoAs_2$, resulting in a lower T_c for the former.

Table IV. Atomic Parameters for Extended Hückel Calculations[a]

atom	orbital	H_{ii}	ζ_{i1} (c_1)	ζ_{i2} (c_2)	ref
Nb	5s	−10.10	1.89		36
	5p	−6.86	1.85		
	4d	−12.10	4.08 (0.6401)	1.64 (0.5516)	
As	4s	−16.22	2.23		37
	4p	−12.16	1.89		

[a] H_{ii} are the orbital ionization energies, ζ_{ij} the Slater exponents, and c_j the coefficients in the double-ζ expansion of the d orbitals.

Thus it appears that the two variables in the exponential term of T_c are related to the band structure description of the $NbAs_2$ structure, and both favor a higher T_c of superconductivity for $MoAs_2$ than for $NbAs_2$. However, the variations in the empirically determined coupling constants are usually small.[26,28,29] As an example, in a family of four organic conducting salts of formula β-$(ET)_2X$, the critical temperatures vary between 1.8 and 8 K, and this variation cannot be explained by the calculated density of states[30] and has been attributed[29] to values of λ in the range $0.43 < \lambda < 0.62$. Hence, it is not likely that the difference of more than 1 order of magnitude between the critical temperatures of superconductivity of $MoAs_2$ and $NbAs_2$ is due only to differences in their electron–phonon coupling constants.

Acknowledgment. Financial support for this research work was generously provided by the DGICYT through Grant PB89-0268. We are grateful to E. Canadell, J. Fontcuberta, and R. Hoffmann for enlightening discussions and to F. Vilardell for the drawings. P.A. thanks the Ministerio de Educación y Ciencia for a Plan Nacional de Nuevos Materiales fellowship.

Appendix: Computational Details

The qualitative theoretical discussions in this paper are based on molecular orbital[31] and tight-binding band calculations[32,33] of the extended Hückel type with a modified Wolfsberg–Helmholz formula,[34] using the atomic parameters shown in Table IV. DOS and COOP diagrams were obtained by averaging throughout the Brillouin zone using a set of 48 k points chosen according to the geometrical method of Ramírez and Böhm.[35] A check calculation with 324 k points gave the same qualitative DOS diagram, including the low-density valley at the Fermi level of $NbAs_2$. An As–H bond distance of 1.52 Å and As–As–H bond angles of 91.8° were used for the model molecule $As_2H_6^{2+}$.

Registry No. $NbAs_2$, 12006-25-6; $MoAs_2$, 12006-24-5.

---

(25) Bardeen, J.; Cooper, L. N.; Schrieffer, J. R. *Phys. Rev.* **1957**, *108*, 1175.
(26) McMillan, W. L. *Phys. Rev.* **1968**, *167*, 331.
(27) Morel, P.; Anderson, P. W. *Phys. Rev.* **1962**, *125*, 1263.
(28) Vonsovsky, S. V.; Izyumov, Yu. A.; Kurmaev, E. Z. *Superconductivity of Transition Metals*; Springer Verlag: Berlin, 1982.
(29) Whangbo, M.-H.; Williams, J. M.; Schultz, A. J.; Emge, T. J.; Beno, M. A. *J. Am. Chem. Soc.* **1987**, *109*, 90.
(30) Williams, J. M.; Beno, M. A.; Wang, H. H.; Geiser, U. W.; Emge, T. J.; Leung, P. C. W.; Crabtree, G. W.; Carlson, K. D.; Azevedo, L. J.; Venturini, E. L.; Schirber, J. E.; Kwak, J. F.; Whangbo, M.-H. *Physica* **1986**, *136B*, 371.
(31) Hoffmann, R. *J. Chem. Phys.* **1963**, *39*, 1397. Hoffmann, R.; Lipscomb, W. N. *J. Chem. Phys.* **1962**, *36*, 2179, 2872, 3489.
(32) Whangbo, M.-H.; Hoffmann, R. *J. Am. Chem. Soc.* **1978**, *100*, 6093.
(33) Whangbo, M.-H.; Hoffmann, R.; Woodward, R. B. *Proc. R. Soc. London, A* **1979**, *366*, 23.
(34) Ammeter, J. H.; Bürgi, H.-B.; Thibeault, J. C.; Hoffmann, R. *J. Am. Chem. Soc.* **1978**, *100*, 3686.
(35) Ramírez, R.; Böhm, M. C. *Int. J. Quantum Chem.* **1988**, *34*, 571. Ramírez, R.; Böhm, M. C. *Int. J. Quantum Chem.* **1986**, *30*, 391.
(36) Summerville, R. H.; Hoffmann, R. *J. Am. Chem. Soc.* **1984**, *106*, 2006.
(37) Underwood, D. J.; Nowak, M.; Hoffmann, R. *J. Am. Chem. Soc.* **1984**, *106*, 2837.